

INITIALIZATION OF 3-D ITERATIVE IMAGE REGISTRATION TECHNIQUES USING POINT MARKERS

Antoine. B. Abche¹, G. S. Tzanakos^{2,3}, E. Micheli-Tzanakou² and E. Karam¹

¹ University of Balamand, Dept of Electrical Engineering
PO box 100, Tripoli, Lebanon

² Rutgers University, Dept. of Biomedical Engineering
Piscataway PO Box 909, NJ 08855

³ University of Athens, Dept of Physics
15771 Athens, Greece

Antoine.abche@balamand.edu.lb

Abstract

Numerous techniques are developed to bring into spatial coincidence two sets of monomodal/multimodal 3-D images acquired by the same/different imaging modalities. Some techniques are based on estimating the transformation parameters using iterative optimization techniques. Since the positioning of the patient is different during each acquisition procedure, the selection of initial values becomes of greater importance so that the minimization algorithms converge to the desired transformation parameters. In other words, if the initial values are not selected appropriately, the registration algorithms could converge to a secondary minimum. In this work, the registration is parameterized in terms of nine parameters, 3 magnifications, three rotation angles (Euler) and three translations. They are estimated by minimizing a chi-square function defined in terms of distances weighted by localization measurement errors of the extracted fiducial external markers using a sequence of non-linear optimization techniques namely, simplex algorithm followed by a gradient approach. The registration approach is initialized using the values estimated by minimizing a cost function in the least square sense. The approach is validated using Monte-Carlo simulation techniques. That is, the residuals (errors) along x, y and z directions and the residuals of distance of regions of interest in the simulated images are evaluated quantitatively and analyzed to study the precision of the registration. The results show that the approach is successful and yields the desired optimum parameters to align the two sets of 3-D data.

Keywords: Registration, Optimization, Multimodal, Imaging modalities, Simulation.

Presenting Author's biography

Antoine Abche. He received the BS degree and MS degree in Electrical Engineering from the University of Toledo (USA) in 1984 and 1986, respectively. He received the PhD degree in Biomedical Engineering from Rutgers The State University (USA) in conjunction with the University of Medicine and Dentistry of New Jersey (Robert Wood Johnson) in 1996. Currently, he is an associate professor in the department of electrical Engineering at the University of Balamand. Dr Abche's research interests are: Virtual Reality, DSP, Image Processing, Analysis and Classification, Telemedicine, Image Registration, Neural Network, Fuzzy Logic, Modeling and System Identification.



1 Introduction

Medical imaging modalities are acquisition systems that provide an ability to see inside the human body in a non-invasive manner. They offer complementary information to radiologists and doctors. While Magnetic Resonance Imaging (MRI) and X-ray Computed Tomography (x-ray CT) are best suited for displaying anatomical and structural information of the organ or Region of Interest (ROI), the functional imaging modalities such as Positron Emission Tomography (PET) and Single Photon Emission Computed Tomography (SPECT) provide information about the function of the corresponding ROI. Since the acquired information is complementary, the integration of anatomical and functional images becomes of great importance in the understanding and interpretation of the latter. Consequently, this illustrates the need to image registration techniques which bring into spatial coincidence the information acquired by mono/multi-modal imaging modalities in the same coordinate system. Various techniques have been developed to tackle this problem and can be found in the literature [1-5]. Broadly, they can be classified into three categories: (1) landmark based on external markers (such as point, reference, frame and head holder) [6, 7, 8] (2) internal landmarks (such as point, curves and surfaces) [9, 10, 11] and (3) intensity based techniques [2, 12, 13, 14].

Several registration techniques are based on iterative optimization techniques to estimate the transformation parameters required to align the collected volume data acquired by the different imaging modalities. The precision of the registration can be affected by several factors such as the identification (manually or automatically) of the corresponding features in the collected images to be registered and the spatial measurement errors associated with the modalities involved. Another factor involves the initialization of such algorithms. Therefore, the latter factor could affect the convergence to the true values of the transformation parameters. Consequently, the initial parameters should be carefully selected. In this context, the convergence of iterative registration algorithms to global or to local optima has been a concern of great importance to researchers in their respective fields. In other words, a good set of values could bring a successful registration with a good precision. Otherwise, the algorithms could converge to a secondary minimum and consequently an error is introduced by overlaying structure (structures) of interest of one modality on location (locations) where it (they) should not be in the coordinate system of the second modality. Therefore, this outlines the need to have a good initial set of parameters that will help an iterative optimization algorithm to estimate the true parameters.

Another reason that emphasizes the need for good initial values is related to the collection of the images.

That is, the images of a particular medical imaging modality are acquired in its respective coordinate system. Such coordinate system is different from one modality to another. In other words, the images collected by different imaging modalities have different coordinate systems. Furthermore, the patient could lie down on the couch of the imaging modality in various positions. Thus, the selection of the initial values (especially if the number of variables to be estimated is high) that could affect the convergence of the registration algorithm becomes a difficult task. In this context, a two-step approach is presented. The first step is performed to acquire some knowledge and information about the initial parameters (starting values) to initialize the iterative minimization technique (second step). This approach is based on external (or internal) point markers that are extracted from the images to be spatially aligned. The initialization step is addressed by performing a linear optimization procedure in the least square sense.

2 Method of Registration

Given two sets of N matched data points $\vec{x}_i = (x_i, y_i, z_i)$ and $\vec{x}'_i = (x'_i, y'_i, z'_i)$ representing the positions vectors in the coordinate systems of modalities 1 and 2, respectively, the registration problem is to estimate the parameters of the transformation that aligns two sets of volume data. The approach assumes that the positions of the external markers in the two modalities are extracted and the correspondence of markers (between the two modalities) is well established. The registration is achieved using two steps: I) the initialization step and ii) the iterative optimization step.

2.1 Initialization step

The initialization step outlines the procedure to estimate the initial values to be fed as initial parameters to the iterative optimization procedure. The transformation from the coordinate system of the first modality to the coordinate system of the second modality is given by

$$\vec{x}' = A \vec{x} + \vec{a} \quad (1)$$

where A is a 3 by 3 matrix given by

$$A = \begin{pmatrix} a_{11} & a_{12} & a_{13} \\ a_{21} & a_{22} & a_{23} \\ a_{31} & a_{32} & a_{33} \end{pmatrix} \quad (2)$$

and $\vec{a} = (a_x, a_y, a_z)$ is the translation vector along x , y and z directions.

Thus, the problem is to estimate the twelve parameters of the overall transformation (nine parameters for the matrix A and three translation parameters) from the 3--D coordinates of two sets of

homologous points in two modalities. The parameters are obtained by minimizing the following cost function

$$\min \|\bar{x}' - (A\bar{x} + \bar{a})\|^2 \quad (3)$$

in the Least Square sense i.e. computing the derivatives of the cost function with respect to the unknown parameters whose values vanish at the minimum [15]. Thus, a χ^2 function is formulated for fitting data from different coordinate systems to estimate the unknown parameters and is defined in terms of distances i.e.

$$\chi^2 = \frac{1}{N} \sum_{i=1}^N (\Delta x_i)^2 + (\Delta y_i)^2 + (\Delta z_i)^2 \quad (4)$$

where $\Delta x_i (= x'_i - \tilde{x}_i)$, $\Delta y_i (= y'_i - \tilde{y}_i)$ and $\Delta z_i (= z'_i - \tilde{z}_i)$ are defined as the residuals of the i 'th marker along x, y and z directions after they are transformed to the same coordinate system (modality 1), respectively. The residual is defined as the difference between the coordinates of the position vector of the i 'th marker $\bar{x}'_i(x'_i, y'_i, z'_i)$ in modality 1 and the position vector of the i 'th marker $\tilde{\bar{x}}_i(\tilde{x}_i, \tilde{y}_i, \tilde{z}_i)$ after transforming the position vector \bar{x}_i (modality 2) to the coordinate system of the position vector \bar{x}'_i (modality 1).

Subsequently, the computation of the derivative of the χ^2 function with respect to the unknown parameter a_{11} yields

$$\frac{\partial \chi^2}{\partial a_{11}} = (-2) \sum_{i=1}^N (x'_i - \tilde{x}_i) \left(-\frac{\partial \tilde{x}_i}{\partial a_{11}} \right) = 0 \quad (5)$$

Similar expressions can be derived for the other unknown parameters. Consequently, a system of linear equations is obtained. The propagation of error is not included because the derivation of the corresponding χ^2 function with respect to the unknown parameters will yield a set of nonlinear equations that can not be solved using linear techniques such as the method of successive elimination.

In this way, the problem is reduced to a system of linear equations. Several methods exist to solve these systems such as Gauss elimination (method of successive elimination), matrix inversion and Lower-Upper triangular decomposition [15]. In this work, the LU technique is implemented to obtain a solution.

2.2 Iterative optimization

The overall affine image transformation from one

coordinate system to the coordinate system of the second modality is defined by:

$$\bar{x}' = R M \bar{x} + \bar{a} \quad (6)$$

where

- i) M is a 3 by 3 magnification matrix that is assumed to be diagonal allowing different magnifications along x, y and z directions. It allows for non-diagonal magnifications by filling the appropriate elements. Therefore, nine parameters in all can be defined for the magnification between two 3-D volume images.
- ii) R is a 3 by 3 orthogonal rotation matrix defined in terms of three rotation angles (Euler angles (α, β, δ)) [16, 17]. The rotation from one coordinate system to another is accomplished via three counterclockwise rotations: α is a rotation angle about the z-axis ($R(\alpha)$), β is a rotation about the new y-axis ($R(\beta)$) and γ is a rotation about the newest z-axis ($R(\gamma)$).
- iii) $\bar{a}(a_x, a_y, a_z)$ is a translation vector along x, y and z directions.

2.3 χ^2 Function Formation

After all marker positions have been transformed to the coordinate system of the same modality, a χ^2 function of the transformation parameters defined in terms of the squares of distances of corresponding markers in two modalities, weighted by the appropriate measurement errors [17], is defined to estimate the unknown parameters. It includes the propagation of errors of a set of markers in one modality to the coordinate system of the second modality. The χ^2 function can be written as:

$$\chi^2 = \frac{1}{N} \sum_{i=0}^N \left[\frac{(\Delta x_i)^2}{(\delta x_i)^2} + \frac{(\Delta y_i)^2}{(\delta y_i)^2} + \frac{(\Delta z_i)^2}{(\delta z_i)^2} \right] \quad (7)$$

where $\Delta x_i (= x'_i - \hat{x}_i)$, $\Delta y_i (= y'_i - \hat{y}_i)$, $\Delta z_i (= z'_i - \hat{z}_i)$ are the residuals of the corresponding i 'th markers along x, y and z directions after registration, respectively, and δx_i , δy_i , δz_i are the combined localization measurement errors of the i 'th corresponding point markers along the x, y and z directions, respectively. The expression of the error δx_i is given by:

$$\delta x_i^2 = (\sigma_{x_i})^2 + (\sigma_{x_i'})^2 \quad (8)$$

$\sigma_{x_i'}$ is estimated from the measurement errors of the i 'th marker in modality 1 along x direction and σ_{x_i} is computed from the measurement errors of the i 'th marker in modality 2 by error propagation methods to modality 1 along the same direction. Thus, the combined localization measurement errors are related to the spatial resolution of the two modalities and depend on the unknown parameters. Similarly, the expressions of δy_i and δz_i can be derived.

2.4 χ^2 Minimization

Since the vector $\vec{\hat{x}}_i$ is the result of the transformation from modality 2 to modality 1, the coordinates $(\hat{x}_i, \hat{y}_i, \hat{z}_i)$ and consequently the residuals $(\Delta x_i, \Delta y_i, \Delta z_i)$ will be a function of the nine transformation parameters. Similarly, the combined measurement errors exhibit the same dependency on these registration parameters. Therefore, the above χ^2 function contains the unknown parameters in such a fashion that cannot lead to a system of linear equations. That is, the registration parameters can not be estimated using matrix inversion techniques. Thus, non-linear iterative minimization techniques are used to determine the parameters of the transformation that are required to align 3-D images acquired by the same/different imaging modalities i.e. the Simplex minimization algorithm [18], followed by a variable Metric Method [19]. The Simplex method provides a very fast convergence to the minimum, whereas the variable metric method is very good when the χ^2 function is near its minimum. The iterative optimization procedure must be initialized by a set of initial values of the parameters to be estimated. The results of the initialization step provide the initialization values to improve the convergence to the global optimum.

3 Method of Evaluation

The evaluation of multimodal 3-D image registration is accomplished by generating simulated images in two modalities as well as images of external markers using Monte-Carlo simulation techniques. Hence, N external markers (in 3-D space) on the face of the simulated head in one modality are generated. Using a predefined transformation (T_0) defined in terms of three Euler angles (α, β, δ), three translations (a_x, a_y, a_z) and three magnifications (M_x, M_y, M_z), each marker position is transformed to a corresponding marker in the second modality. Then, each marker position is randomly perturbed from its 3-D original position using Gaussian measurement errors simulating marker localization errors. The markers are independently

perturbed in each modality and along each direction x , y and z . At this stage, the proposed approach is performed (two stages) to recover the original parameters of the transformation (T_{init} (first stage) and T_{opt} (second stage)). At this point, Monte-Carlo simulated images are formed by generating a large number of 3-D space coordinates of points $P(x, y, z)$ distributed inside the region of interest such that the density of points will be proportional to, and therefore are representative of, the activity distribution $f(x, y, z)$ within the image. These 3-D points (each defined by its spherical coordinates (r, θ, ϕ)) are treated in the same way as the fiducial point markers, but are not used in the registration process (i.e. estimation of the parameters). Thus, assuming the same known transformation parameters (T_0), the "image" is transformed to modality 2. By introducing the point localization errors (Gaussian distribution), the "images" are smeared in the two modalities. This is done by altering the coordinates of each point randomly and in accordance to the spatial resolution of the corresponding modality. At this stage, the images of an object in two modalities are simulated. By using the estimated values of the transformation parameters (T_{init} and T_{opt}), the "image" of modality 2 is transformed to the coordinate system of modality 1. Since the correspondence between test points in the two "images" is known, the residuals $\Delta X, \Delta Y, \Delta Z$ and ΔD can be formed. At this point, the dependence of the residuals on the position inside the image of the simulated head as well as other aspects of 3-D image registration (such as the effect of the combined localization errors in the two modalities, the number of external markers and their positions) can be quantitatively studied and evaluated.

4 Simulation and Results

In this experiment, the head is assumed to be spherical of radius $R=10$ cm. The coordinate system (Figure 1) is right handed with the $+x$ axis ($\theta=90^\circ, \phi=0^\circ$) coming out of the ear, the $+y$ axis ($\theta=90^\circ, \phi=90^\circ$) going through the nose and the $+z$ axis ($\theta=0^\circ$) going through the top of the head. Each point in the image is represented by its spherical coordinates (r, θ, ϕ) .

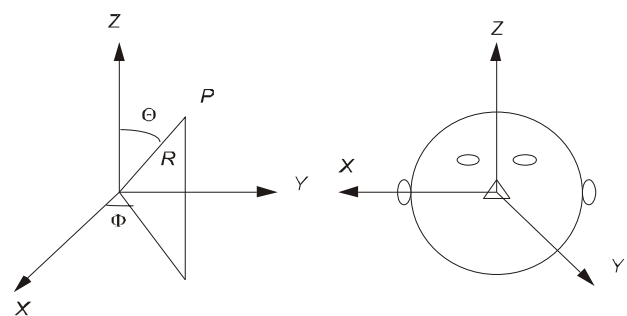


Figure 1: coordinate system of Modality 1

The markers are assumed to be on the face of the patient ($0^\circ < \phi < 180^\circ$). The spatial localization measurement errors in the two modalities (σ_1, σ_2) are assumed to have values equal to 2 and 5 mm. These values are used to introduce noise randomly and independently in each modality and along each axis in the respective coordinate system. The Monte-Carlo experiments are performed for various numbers of external point markers. In these simulations, the assumed head is divided into regions defined by ranges of the spherical coordinates (r, θ, ϕ). The angle θ that varies from 0° to 180° , is divided into 6 segments, each corresponds to 30° . The azimuthal angle ϕ that varies from 0° to 360° , is divided into 12 segments, each corresponds to 30° . The radius is divided into 3 segments; each corresponds to $10/3$ cm. However, the radius is divided into 10 segments (each segment has a range of 1 cm), to study the effect of the radius on the mean residual ΔD of various regions of the Monte-Carlo simulated head.

Figures 2 and 3 show the mean ΔD for various numbers of external markers (N) for two different regions of the simulated head: (1) a region in front of the head ($60^\circ < \theta < 90^\circ$, $60^\circ < \phi < 90^\circ$ and $6.67 < r < 10$ cm) and (2) a region in the back of the head ($60^\circ < \theta < 90^\circ$, $240^\circ < \phi < 270^\circ$ and $6.67 < r < 10$ cm), respectively. Two plots are presented in each figure. They correspond to the results obtained after the initialization procedure (Blue) and after the iterative optimization procedure (Violet). The results show that the initialization procedure always yields a set of parameters that is close to the desired parameters if the system has enough degree of freedom ($N \geq 4$). On the other hand, a comparison with the iterative optimization procedure shows that the mean residuals ΔD of the same ROI are larger after the implementation of the initial procedure, especially in the regions located in the back of the head (furthest away from the location of the markers used in the estimation process of the registration parameters). Thus, the precision of the registration is much better after the iterative optimization procedure is performed. This difference is attributed to the fact that the correlation between the rotation parameters is not taken into consideration in the system of linear equations (initialization step). However, this effect will be reduced as the number of external point markers is increased. Consequently, the precision of the two stages will be similar.

Furthermore, by analyzing a particular step (initialization or iterative optimization) for a given set of corresponding point markers, it can be observed that the precision of the registration is much better in the regions that are located in front of the head. This is reflected in smaller residuals ΔD after the corresponding external point markers are transformed to the same coordinate system (Figures 2 and 3). This is due to the fact that the point markers used to estimate the respective transformation are located in

front of the simulated head. Consequently, they are close to the regions of interest. In other words, the closer the region of interest to the location of markers used in the initialization and optimization procedures, the better is the corresponding precision. On the other hand, the regions in the back of the assumed head exhibit the worst precision.

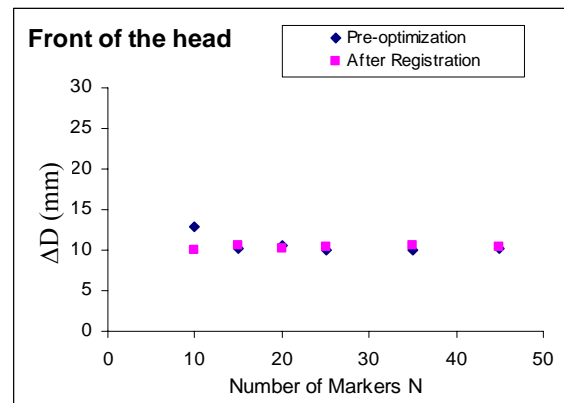


Fig 2: Mean ΔD for various N : a) after initialization procedure b) after registration for a region located in front of the simulated head ($60^\circ < \theta < 90^\circ$, $60^\circ < \phi < 90^\circ$ and $6.67 < r < 10.0$ cm).

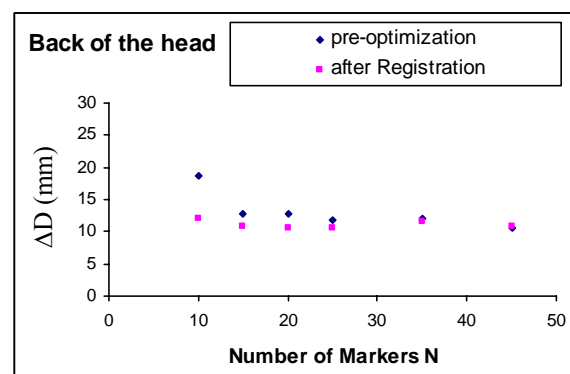


Fig 3: Mean ΔD for various N : a) after initialization procedure b) after registration for a region located in the back of the simulated head ($60^\circ < \theta < 90^\circ$, $270^\circ < \phi < 300^\circ$ and $6.67 < r < 10.0$ cm).

The corresponding σ_{rms} for the same ranges of radius, polar and azimuth angles are illustrated in Figures 4 and 5, respectively. The results are almost similar i.e. the results of the pre-optimization and iterative optimization steps for various numbers of markers. However, a certain difference is observed in the regions located closer to the surface of the simulated head for N less than 10. On the other hand, a larger difference is observed for the regions located in the back of the head (especially $N < 10$). However, a smaller difference persists until the number of external point markers reaches a value of 20. Similar conclusions can be deduced by studying the precision of the registration in other regions of the Monte-Carlo simulated head.

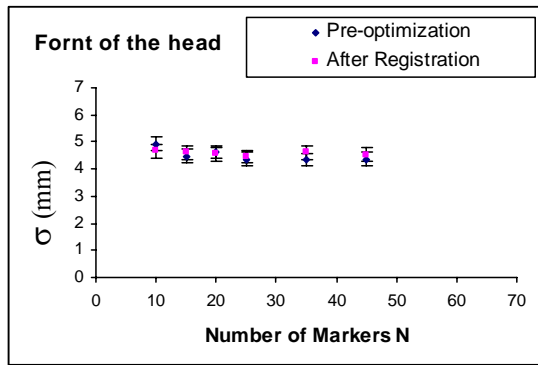


Fig 4: Standard deviation σ_D for various N: a) after initialization procedure and b) after registration for a region in the front of the simulated head ($60^\circ < \theta < 90^\circ$, $60^\circ < \phi < 90^\circ$ and $6.67 < r < 10.0$ cm).

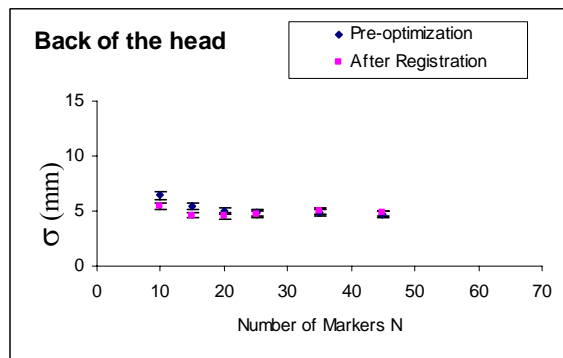


Fig 5: Standard deviation σ_D for various N: a) after initialization procedure and b) after registration for a region in the front of the head ($60^\circ < \theta < 90^\circ$, $270^\circ < \phi < 300^\circ$ and $6.67 < r < 10.0$ cm).

Figures 6 and 8 show the dependence of the mean ΔD on the radius r (cm) for two different regions within the simulated head: (1) a region bounded by the following ranges of spherical coordinates $60^\circ < \theta < 90^\circ$, $60^\circ < \phi < 90^\circ$ and 2) a region defined by $60^\circ < \theta < 90^\circ$, $240^\circ < \phi < 270^\circ$. Two graphs are illustrated in each Figure. While one graph corresponds to the precision of the registration after the pre-optimization procedure is performed (Blue), the second graph shows the precision of the registration of the overall procedure (Violet). The number of external point markers used to achieve the 3-D image registration is assumed to be 15. The corresponding standard deviation σ_{rms} , defined for the same ranges of the azimuth and theta angles are illustrated in Figures 7 and 9, respectively.

Since the origin of the coordinate system is assumed to be at the center of the simulated head, a smaller value of r implies that the corresponding region is closer to the center of the head. Subsequently, the higher the value of r is, the closer the corresponding region is to the surface. Thus, due to the selected

values of θ and ϕ , Figure 6 reflects the effect of r on the precision of the registration as the region of interest is moving from the center of the head toward the surface where the point markers are located i.e. the front of the simulated head. On the other hand, Figure 8 reflects the dependence of the mean residual ΔD on the radius as the region of interest is moving from the center of the head toward the surface where the point markers are not located i.e. the back of the simulated head.

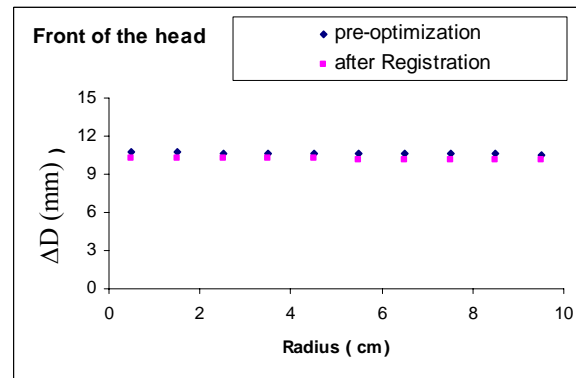


Fig 6: The dependence of mean ΔD on the radius r (cm): a) after initialization procedure b) after registration for a region defined by $60^\circ < \theta < 90^\circ$ and $60^\circ < \phi < 90^\circ$.

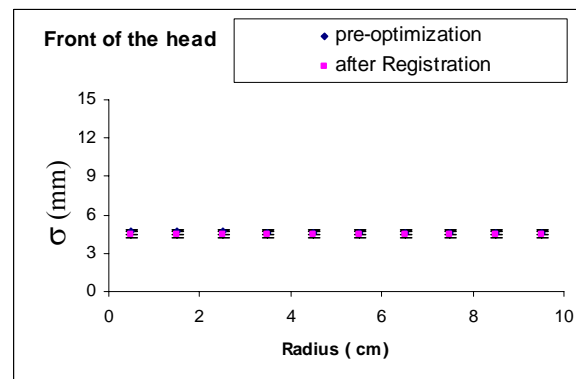


Fig 7: Dependence of the standard deviation σ_D on the radius r (cm): a) after initialization procedure and b) after registration for a region defined by $60^\circ < \theta < 90^\circ$ and $60^\circ < \phi < 90^\circ$.

The results show that the precision of the registration is better for the regions of the simulated head that are closer to the location of the point markers. That is clearly evident in the two figures illustrating the dependence of the mean residual ΔD on the radius. In other words, Figure 6 shows that the mean residual decreases as the radius increases. Figure 8 illustrates that the worst precision is observed in the region that is closer to the surface in the back of the simulated

head i.e. mean ΔD increases as the radius increases. This trend is observed after each individual registration step is performed (i.e. pre-optimization and the iterative optimization). On the other hand, the pre-optimization procedure presents the worst precision when it is compared with the precision of the overall approach for all various regions. This observation is more evident in the region of the back of the head (i.e. $180^\circ < \phi < 360^\circ$ - Figure 8). On the other hand, the location of the point markers in front of the simulated head ($0^\circ < \phi < 180^\circ$) tends to minimize the difference between the residuals ΔD of the corresponding regions as illustrated in Figure 6.

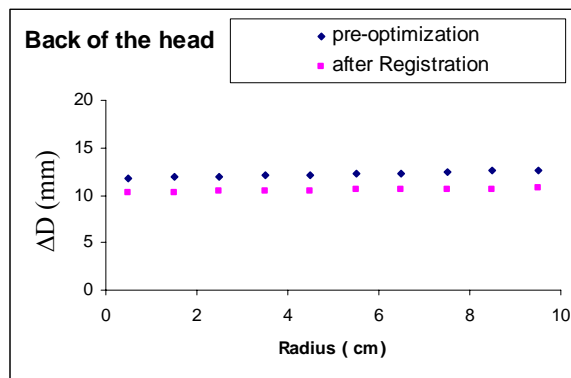


Fig 8: The dependence of mean ΔD on the radius r (cm): a) after initialization procedure b) after registration for a region defined by $60^\circ < \theta < 90^\circ$ and $270^\circ < \phi < 300^\circ$.

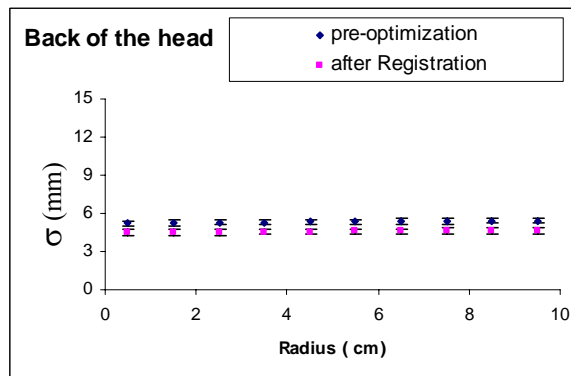


Fig 9: Dependence of the standard deviation σ_D on the radius r (cm): a) after initialization procedure and b) after registration for a region defined by $60^\circ < \theta < 90^\circ$ and $270^\circ < \phi < 300^\circ$.

Furthermore, the small difference between the residuals ΔD in front of the head (Figure 6) can also be attributed to the fact that the effect of the correlation between the rotation parameters ($N=15$) is not as large as the case of a lower number of external point markers. Thus, the precision of the two

registration methods will be almost comparable. However, the coupling effect of the rotation parameters embedded in the pre-optimization procedure does not have the same effect on the regions where the point markers are not located. Therefore, a bigger difference is observed (Figure 8). This effect is minimized for a higher number of markers as already presented earlier (Figures 2 and 4).

With respect to the corresponding standard deviations, the results are comparable in the regions corresponding to the front of head (Figure 7). That is, the corresponding values, obtained by both stages of registration, are almost the same. This could be due to the location of point markers and the smaller effect of the coupling of rotation variables as outlined earlier. On the other hand, this effect becomes more apparent in the regions corresponding to the back of the simulated head (Figure 9). That is, a bigger difference is observed between the results of the two steps. Furthermore, the $\sigma_{\Delta D}$ is increased as the radius is increased (Figure 9). However, a smaller decrease is observed as the region of interest is moving toward the surface located in front of the simulated head (Figure 7).

5 Conclusion

Iterative registration algorithms require a set of initial values of the parameters as an input. These values can affect the convergence of such algorithms to the desired registration parameters. Furthermore, the different positioning of the patient during each acquisition procedure underlines the importance of the selection of these values. Consequently, this may lead to improve the performance and the accuracy of the registration techniques to align two sets of 3-D images acquired by the same/different medical imaging modalities

In this work, a two-phase registration approach, an initialization procedure followed by an iterative optimization procedure, is presented. The first step is based on the minimization of an error function in the least square sense. Then, the results of the latter step are fed as input to the second stage i.e. the iterative optimization step (the simplex algorithm followed by a variable metric Method). The presented approach is validated using Monte-Carlo simulation techniques i.e. simulated images of the head are generated as well as images of the external point markers in two modalities to study quantitatively the precision of the registration.

The results show that the approach is successful and yields the desired optimum parameters to align the two sets of 3-D data. Even though the first estimation is asymptotically biased, it is generally close to the global optimum when a high degree of freedom exists ($N \geq 4$). Furthermore, the precision of the registration is much better for a region in front of the head where

the external point markers are located. On the other hand, the worst precision is achieved in the regions located in the back of the simulated head. This observation is made for the initialization step as well as for the overall registration procedure. However, the second step always leads to a better precision for the same corresponding region i.e. minimum residual ΔD .

6 References

- [1] D. L. Hill, P. G. Batchelor, M. Holden & J. Hawkes. Medical Image Registration. *Phys. Med. Biol.*, Vol. 46, pp. 1-45, 2001.
- [2] J. P. W. Pluim, J. B. A. Maintz and M. A. Viergever. Mutual Information-based Registration of medical Images A Survey. *IEEE Transaction On Medical Imaging*, Vol. 22, No 8, pp 986-1004, 2003.
- [3] L. G. Brown. A Survey of Image Registration Techniques. *ACM Computing Surveys*, Vol. 24, No. 4, pp. 325-376, 1992.
- [4] J. B. A. Maintz and M. A. Viergever. A Survey of Medical Image Registration. *Med. Image Anal.*, Vol. 2, 1-36, 1998.
- [5] H. Lester and S. Arridge. A Survey of Hierarchical Nonlinear Medical Image Registration. *Pattern Recognition*, Vol. 32, No 1, pp 129-149, 1999.
- [6] A. B. Abche, G. S. Tzanakos, E. Micheli-Tzanakou. Evaluation of 3-D Image Multimodal Registration Techniques Using Monte-Carlo Simulated 3-D Images. *3rd conference on modeling and Simulation in Biology, Medicine and Biomedical Engineering*, Lebanon, 27-30 May, 2003.
- [7] Mark W. Wilson and James A. Mountz. A reference system for neuro-anatomical localization on functional reconstructed cerebral images. *Journal of Computer Assisted Tomography*. Vol. 13, No. 1, pp. 174-178, 1989.
- [8] George S. Tzanakos, Antoine B. Abche, Evangelia Micheli -Tzanakou, Theodore Stahl, Xiaoming Wan and Tony Yudd. Multimodal 3-D Image Registration of MRI - SPECT Volume Images. *World Congress 2000, IEEE – EMBS*, paper # 5886-26335, Chicago, 23-28 July 2000.
- [9] Antoine B. Abche, Elie, Tohme, Toufic El Chaer, Elie Karam, Hamam Yskandar, Michel Bouchoucha and François Rocaries. Image Registration of Radiographic Images Using an Elastic Approach. *IEEE Nuclear Science Symposium and Medical Imaging Conference*, San Diego, USA, pp. 2081-2085, 29 Oct - 5 Nov, 2006.
- [10] Minghui Xia, and Bede Liu. Image Registration Using Super Curves. *IEEE Transactions on Image Processing*, Vol. 13, No. 5, pp. 720-732, 2004.
- [11] Charles A. Pelizzari, George T. Y. Chen, Danny R. Spelbring, Ralph R. Weichselbaum and Chin-Tu Chen. Accurate three dimensional registration of CT, PET, and/or MR images of the brain. *Journal of Computer Assisted Tomography*, Vol. 13, No. 1, pp. 20-26, 1989.
- [12] Antoine Abche, Fadi Yaacoub, Aldo Maalouf and Elie Karam. Image Registration based on Neural Network and Fourier Transform. *IEEE Engineering in Medicine and Biology Conference (EMBC'2006)*, New York, USA, pp. 4803-4806, August 31- September 4, 2006.
- [13] Philippe Thevenaz. Urs E. Ruttimann and Michael Unser. A Pyramid Approach to Sub-Pixel Registration Based on Intensity. *IEEE Transactions on Image Processing*, Vol. 7, No. 1, pp. 27-41, 1998.
- [14] R. P. woods, S. R. Cherry and J. C. Maziotta. Rapid Automated Algorithm for aligning and Reslicing PET Images. *Journal of Computer Assisted Tomography*, Vol. 16, No. 4, pp. 620-633, 1992.
- [15] Joel N. Franklin. Matrix Theory. Prentice-Hall, inc., Englewood Cliffs, New Jersey, 1988.
- [16] George Arfken. Mathematical methods for physicists. Second edition, Academic Press, N.Y., 1971.
- [17] A. B. Abche, G.S. Tzanakos and E. Micheli-Tzanakou. A New Method for Multimodal 3-D image Registration with External Markers. *Nucl. Sci. symp. and Med. Imag. Conf.*, Oct 30-Nov5, pp. 1822-1826, 1994.
- [18] J. A. Nelder & R. Mead. A Simplex Method for Function Minimization. *Computer Journal*, Vol. 7, pp. 308-313, 1965.
- [19] R. Fletcher and M. J. D. Powell. A Rapidly Convergent Descent Method for Minimization. *Computer Journal*, Vol. 6, pp. 163-168, 1963.